J|A|C|S
COMMUNICATIONS

Published on Web 02/13/2003

# Synthesis of Unidirectional Alumina Nanostructures without Added Organic Solvents

Hyun Chul Lee,[†] Hae Jin Kim,[‡,§] Soo Hyun Chung,[||] Kyung Hee Lee,[†] Hee Cheon Lee,[‡] and Jae Sung Lee*,[†]

*Department of Chemical Engineering and Department of Chemistry and Division of Molecular and Life Science, Pohang University of Science and Technology, Pohang, 790-784, Republic of Korea, Korea Basic Science Institute, Daejeon, 350-333, Republic of Korea, and Korea Institute of Energy Research, Daejeon, 305-343, Republic of Korea*

Received November 27, 2002; E-mail: jlee@postech.ac.kr

Aluminum oxide is most commonly used as adsorbents, catalysts, and catalyst supports. Recently, efforts have been devoted to the synthesis of nanostructured alumina with an ordered pore structure. The most common synthetic strategy for such materials is based on templating of surfactant micelle structures. The typical hydrothermal synthesis based on supramolecular surfactant assembly yields mesoporous alumina molecular sieves with a wormholelike channel motif.[1−6] The synthesis of nanostructured alumina with other geometries has also been reported. Zhu et al. reported the $\gamma$-alumina nanofibers prepared from aluminum hydrate with poly(ethylene oxide) surfactants.[7] Zhang et al. synthesized porous lath- to rod-shaped nanoparticles with a nonionic surfactant.[8] There has been no report on the synthesis of hollow alumina nanotubes based on templating of surfactants, although electrochemical anodizing methods are known to produce individual and branchy alumina nanotubes.[9,10]

The syntheses of nanostructured materials based on surfactant templating are generally conducted in aqueous or nonaqueous solvents to disperse reactants. However, we report here a new synthetic route of thermally stable alumina nanostructures without the addition of any organic solvent. The salient feature of this procedure is the production of unidirectional nanostructures (denoted as P-ANS-x, POSTECH-Alumina NanoStructures, where x = $S^+$ for cationic, $S^-$ for anionic, S° for neutral, and N° for nonionic surfactant) such as nanotubes, nanofibers, and nanorods depending on the nature of the employed surfactants.

The details of the P-ANS nanostructure preparation are as follows: distilled water (160 mmol) was added very slowly to a homogeneous mixture of surfactant (40 mmol) and aluminum tri-*sec*-butoxide (80 mmol) without any organic solvents while stirring. The molar composition of the resulting gel, therefore, was 0.5:1:2 for surfactant:Al:water. After being stirred until the homogeneity was obtained, the resulting well-mixed gel was put into a Teflon-lined autoclave vessel. The hydrothermal reaction was then followed at 423 K for 72 h under autogenous pressure and static condition. The product was washed several times with absolute ethanol, dried sequentially at room temperature for 16 h and at 383 K for 5 h, and then calcined at 773 K for 4 h in the flow of air.

In the presence of 1-butanol as an organic solvent (800 mmol) with the mixture of a cationic surfactant and an aluminum precursor (aluminum tri-*sec*-butoxide), the hydrothermal synthesis yielded mesoporous alumina molecular sieves (Figure 1A) with a wormholelike morphology as reported earlier.[1,4] Synthesis under the same conditions with the same surfactant and aluminum precursor, but without the added organic solvent, gave a product with a distinct unidirectional fibrous morphology. This demonstrates a profound effect of organic solvents in the hydrothermal synthesis of alumina on the morphology of the obtained products.

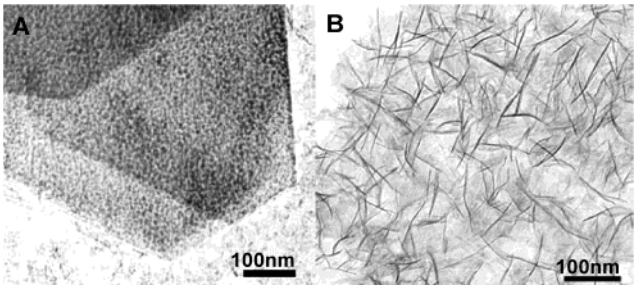


***Figure 1.*** TEM images of the hydrothermally synthesized alumina materials after calcination at 773 K: (A) using 1-butanol as an organic solvent ($S_g$ = 400 $m^2$/g), (B) without added solvent ($S_g$ = 385 $m^2$/g).

A field emission high-resolution transmission electron microscopy (FE-HREM) study of the P-ANS materials has been carried out to probe the detailed architecture of the nanostructured alumina. The low magnification TEM images in Figure 2A, C, E, G show that all samples assume unidirectional nanostructures with a quite regular diameter and a length over 200 nm. Uncalcined samples containing surfactants also showed similar morphologies, indicating that the morphologies had been determined during the hydrothermal reaction stage by interaction between aluminum butoxide and the surfactants.

Samples prepared from cationic and nonionic surfactants (P-ANS-$S^+$ and P-ANS-N°) showed isolated individual and branched nanotubes. In contrast, the HR-TEM image of P-ANS-$S^-$ shows thickets of densely distributed nanofibers with a 3 nm diameter. Finally, P-ANS-S° shows nanorods of 18 nm in diameter and 180 nm in length. A rod in Figure 2H shows stripelike fringes equally spaced by ca. 3 nm in parallel with the direction of the rod axis. These results indicate that the different surfactant micelles induce the different structures probably due to the different modes of interaction with the aluminum precursor. The selected-area electron diffraction (SAED) patterns taken from a region of P-ANS (Figure 2, insets) show spot patterns superimposed with diffuse ring patterns which correspond to the reflection of crystalline aluminum oxide along the nanostructure framework.

Displayed in Figure 3 are the wide-angle range powder X-ray diffraction (XRD) patterns for the mesophases containing various surfactants and the alumina products after removal of surfactants

[†] Department of Chemical Engineering, Pohang University of Science and Technology.
[‡] Department of Chemistry and Division of Molecular and Life Science, Pohang University of Science and Technology.
[§] Korea Basic Science Institute.
[||] Korea Institute of Energy Research.


**10.1021/ja029494l CCC: $25.00** 

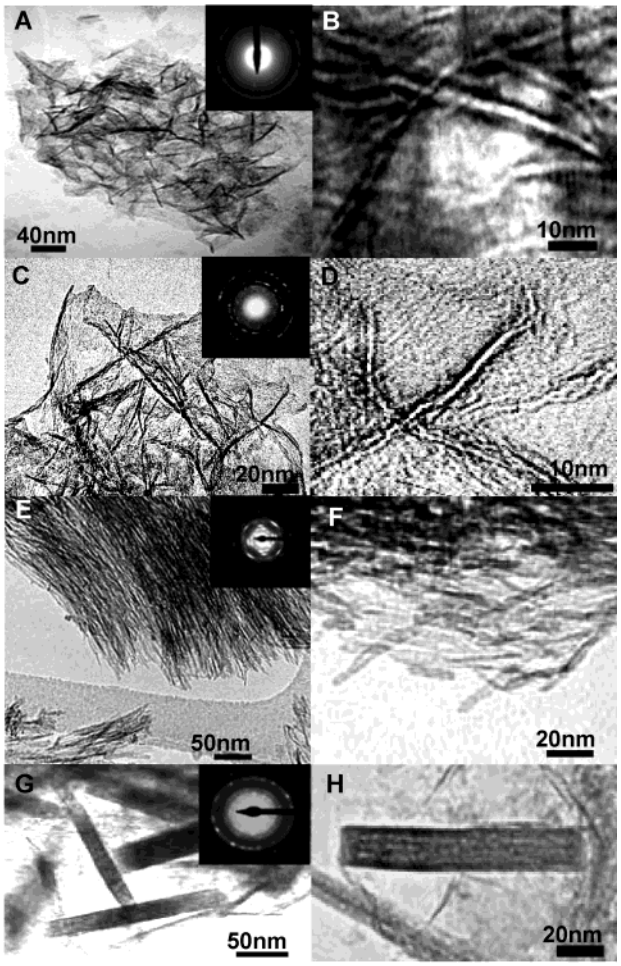


***Figure 2.*** High-resolution transmission electron microscopy (HR-TEM) images of the calcined alumina nanotubes: (A, B) P-ANS-$S^+$ for cationic surfactant, (C, D) P-ANS-N° for nonionic surfactants, (E, F) P-ANS-$S^-$ for anionic surfactant, (G, H) P-ANS-S° for neutral surfactant, (B, D, F, H) FE-HREM for P-ANS materials.

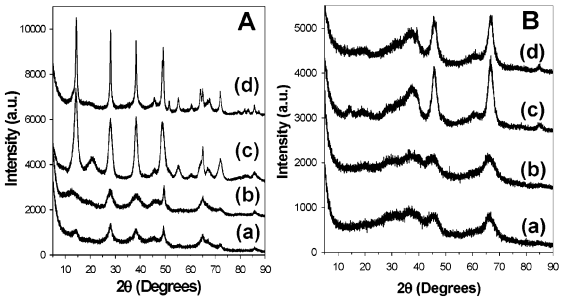


***Figure 3.*** X-ray diffraction patterns for alumina nanostructures: (A) uncalcined samples, (B) calcined samples, (a) P-ANS-$S^+$, (b) P-ANS-N°, (c) P-ANS-$S^-$, (d) P-ANS-S°.

by calcination at 773 K. The mesophase exhibited the XRD powder patterns of boehmite, whereas calcined products showed those of $\gamma$-alumina. Thus, nanostructured boehmite/surfactant precursors are converted to $\gamma$-alumina during calcination without much change in morphology. The materials synthesized with anionic and neutral surfactants showed the better-crystalline boehmite and $\gamma$-alumina phases. The difference correlates with different morphologies shown

***Table 1.*** Textural Properties of P-ANS Alumina Nanostructures Calcined at 773 K for 4 h

| materials | surfactant | BET $S_g$ ($m^2/g$) | BJH pore size (nm) | pore volume ($cm^3/g$) |
|---|---|---|---|---|
| P-ANT-$S^+$ | $CH_3(CH_2)_{15}N(CH_3)_3-Br$ | 385 | 3.7 | 0.77 |
| P-ANT-N° | $CH_3(CH_2)_{15}-(PEO)_2-OH$ | 445 | 3.0 | 0.73 |
| P-ANT-$S^-$ | $CH_3(CH_2)_{14}COOH$ | 282 | 2.8 | 0.34 |
| P-ANT-S° | $CH_3(CH_2)_{15}NH_2$ | 300 | 2.8 | 0.52 |

in Figure 2. The materials maintained their $\gamma$-alumina phase up to 1323 K. The $^{27}Al$ MAS NMR spectra showed a tetrahedral to octahedral aluminum ratio of ca. 1:3 without any pentavalent aluminum. Thus, all P-ANS materials prepared with various surfactants appear to be made of crystalline $\gamma$-alumina walls.

The textural properties of P-ANS are summarized in Table 1. The P-ANS showing tubular morphology exhibited higher surface areas and pore volumes. Although nanorod alumina showed particularly low surface area, pore volume, and pore size, these values could be rationalized only when we assume that the rod contains internal pores of ca. 2.8 nm. This interpretation is supported by the TEM image in Figure 2H.

In the surfactant/water/butanol system, it is expected that the cylindrical surfactant micelle is formed and the alumina precursor condenses around it according to the well-established templating mechanism. The mesoporous alumina molecular sieve is synthesized with a wormholelike channel structure under this condition. Without added organic solvent, however, unidirectional nanostructures are formed probably through a mechanism similar to those proposed for the formation of silica nanotubes[11] and alumina nanofibers.[7] By this mechanism, an interaction between surfactant and boehmite surfaces allows the boehmite crystallites to grow along one direction to give a fibrous morphology. Further assembly into bundles would yield either a thicket of fibers or a nanorod of larger sizes depending on the nature of surfactant. In any case, these nanotubes, nanofibers, and nanorods show unique morphologies that have never been reported before for alumina. We also found that this synthetic procedure could be applied to the synthesis of nanostructures of other oxides such as titanium oxide.

**Acknowledgment.** This work has been supported by the BK-21 program of the Korea Ministry of Education and the Research Center for Energy Conversion and Storage and NRL programs of the Korea Ministry of Science and Technology.

**References**

(1) Bagshaw, S. A.; Pinnavaia, T. J. *Angew. Chem., Int. Ed. Engl.* **1996**, *35*, 1102.
(2) Vaudry, F.; Khodabandeh, S.; Davis, M. E. *Chem. Mater.* **1996**, *8*, 1451.
(3) Yada, M.; Machida, M.; Kijima, T. *Chem. Commun.* **1996**, 769.
(4) Cabrera, S.; Haskouri, J. E.; Alamo, H.; Beltrán, A.; Beltrán, D.; Mendioroz, S.; Marcos, M. D.; Amorós, D. *Adv. Mater.* **1999**, *11*, 379.
(5) Valange, S.; Guth, J.-L.; Kolenda, F.; Lacombe, S.; Gabelica, Z. *Microporous Mesoporous Mater.* **2000**, *35*−*36*, 597.
(6) González-Peña, V.; Días, I.; Márques-Alvarez, C.; Sastre, E.; Pérez-Pariente, J. *Microporous Mesoporous Mater.* **2001**, *44*−*45*, 303.
(7) Zhu, H. Y.; Riches, J. D.; Barry, J. C. *Chem. Mater.* **2002**, *14*, 2086.
(8) Zhang, Z.; Hicks, R. W.; Pauly, T. R.; Pinnavaia, T. J. *J. Am. Chem. Soc.* **2002**, *124*, 1592.
(9) Pu, L.; Bao, X.; Zou, J.; Feng, D. *Angew. Chem., Int. Ed.* **2001**, *40*, 1490.
(10) Zou, J.; Pu, L.; Bao, X.; Feng, D. *Appl. Phys. Lett.* **2002**, *80*, 1079.
(11) Adachi, M.; Harada, T.; Harada, M. *Langmuir* **2000**, *16*, 2376.

JA029494L